# Influence of the copper coordination spheres on the N2Or activity of a mixed-valent copper complex containing a Cu2S core

Charlène Esmieu, Maylis Orio, Stéphane Ménage, Stéphane Torelli

# Influence of the copper coordination spheres on the $N_2Or$ activity of a mixed-valent copper complex containing a $\{Cu_2S\}$ core.

*Charlène Esmieu,[†] Maylis Orio,[‡] Stéphane Ménage,[†] Stéphane Torelli*[*,†]*

[†] CEA-DRF-BIG-LCBM-BioCE, Univ. Grenoble Alpes, CNRS UMR 5249, 17 rue des Martyrs, 38054 Grenoble, France

[‡] Institut des Sciences Moléculaires de Marseille, Aix Marseille Université, CNRS, Centrale Marseille, $ISM_2$ UMR 7313, 13097, Marseille, France

## INTRODUCTION

Nitrous oxide ($N_2O$) is an aggressive pollutant due to its major greenhouse effect and global warming potential (GWP, 300 times that of $CO_2$).[1] Besides natural emissions, anthropogenic $N_2O$ sources mainly rely on agricultural activities, nitric / adipic acids factories and transportations. Independently, Health issues have been connected with long-term $N_2O$ exposures.[2] Among the identified effects or consequences, one can cite the inactivation on methionine synthase[3], as well as genetic[4] or cerebrocortical damages.[5] Consequently, mitigation of the $N_2O$ levels using efficient remediation catalysts or elaboration of selective sensors constitute important scientific breakthroughs.

Despite its chemical inertness, $N_2O$ reduction is a thermodynamically favorable process ($N_2O + 2H^+ + 2e^- \rightarrow N_2 + H_2O$, $E° = 1.35$ V @ pH 7.0 *vs* NHE) that Nature masters with the so-called copper-containing enzyme nitrous oxide reductase ($N_2Or$) during the denitrification pathway.[6] This reactivity is remarkable since the 59 kcal/mol (gas phase) energy barrier for the N-O cleavage are overcome under physiological conditions. $N_2Or$ is a homodimer containing two different copper motifs: a dinuclear $Cu_A$ site acting as electron mediator and a tetranuclear $Cu_4S$ cluster for $N_2O$

reduction. To date, two different structures are known for the $Cu_4S$ active site, depending on purification methods. The first, $Cu_Z^*$, is isolated under aerobic conditions while the second, $Cu_Z$, is obtained in reductive medium (Chart 1).[7] The main difference lies in the open $Cu_I$-$Cu_{IV}$ edge with coordinated hydroxide/water or sulfide ions. Deep experimental investigations combined with computational methods provided a major knowledge to clarify the reaction mechanism.[8] Indeed, a better understanding of how $N_2$Or activates and reduces $N_2O$ would contribute to the perspectives described above. The involvement of a Cuz° intermediate with a μ,1-3 coordination mode for $N_2O$ at the $Cu_I$-(μ,S)-$Cu_{IV}$ edge, together with the participation of a hydrogen bond with a neighboring lysine residue to favor the N-O bond cleavage, has been proposed.[9]

In our group, we aim at developing bio-inspired $Cu_2S$-containing complexes representative of the truncated active $Cu_4S$ native cluster to propose structure/activity correlations for $N_2O$ activation/reduction. In the literature, few examples of $Cu_x$-$S_y$ (x = 2-4 and y = 1, 2) architectures have been reported for stoichiometric $N_2O$ reduction at low temperature (-80°C).[10] We already demonstrated that mixed-valent (MV) dicopper (I,II) cores embedded in a thiophenolate-containing ligand can reduce $N_2O$ under single turnover conditions depending on the metal ions environments at room temperature and under $N_2O$ atmospheric pressure. Indeed, while **[1]**,[11c] **[3]**[11a] and **[4]**[11a] are inactive, **[2]**[11b] exhibits a unique $N_2$Or activity (Chart 1). These results point out *(i)* the need of exchangeable position(s) for the reactivity and *(ii)* the importance of one of the exogenous coordinated ligand since one position has to be occupied by a water molecule (Cu-$OH_2$ motif).

Here, we demonstrate that the coordination sphere of the Cu-X part adjacent to Cu-$OH_2$ within a given dinuclear complex significantly affects the kinetic at a single turnover level. Indeed, the introduction of an acetonitrile ligand for **[5]** (generated by dissolving **[3]** in acetone and fully characterized in this study) in place of a triflate ion in **[2]** results in a 10 times faster reduction

process. A nitrogen-rich environment, as present in native $N_2Or$, thus appears more prone to facilitate the reaction.

**Chart 1.** Representation of the $N_2Or$ active sites and chemical structures of MV **[1]**, **[2]**, **[3]**, **[4]** and **[5]**. The main differences within $Cu_2S$ cores are highlighted in red; $OTf^-$ stands for trifluoromethanesulfonate anion.

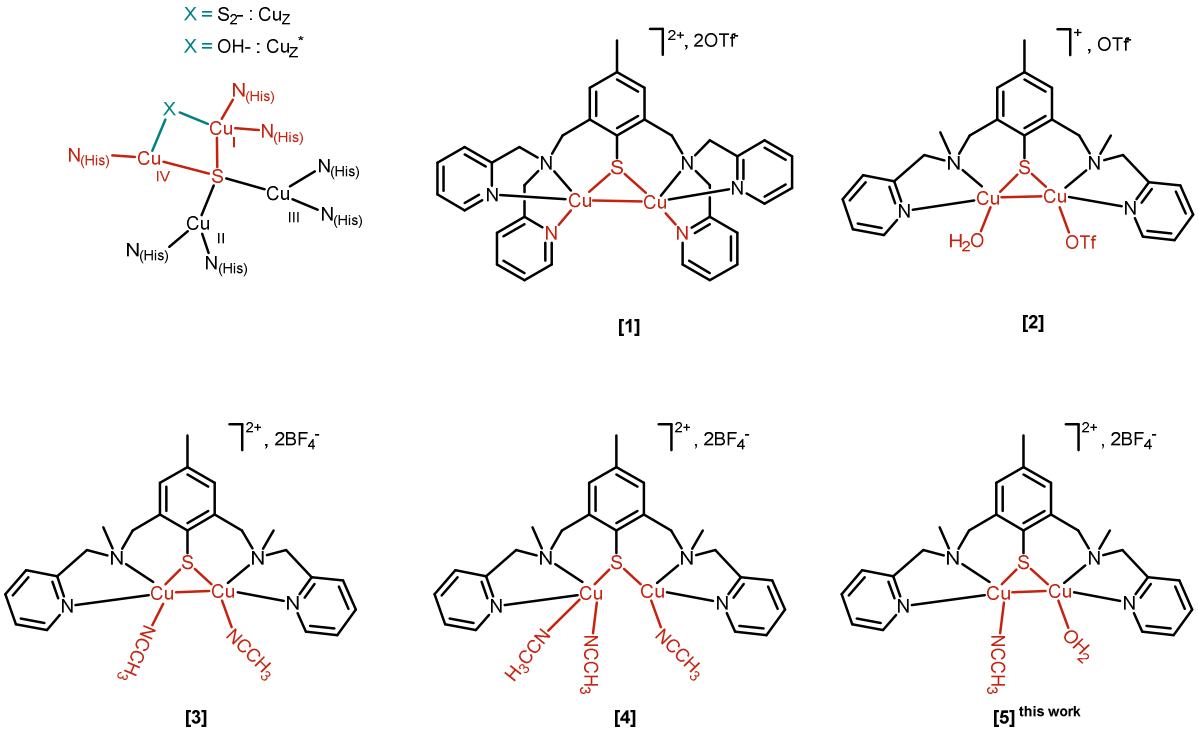


## RESULTS AND DISCUSSION

The UV-vis/NIR spectrum recorded upon dissolution of crystalline **[3]** in acetone lead to an intense purple solution with features at 1205 nm ($\varepsilon$ = 760 $M^{-1}.cm^{-1}$), 775 nm ($\varepsilon$ = 855 $M^{-1}.cm^{-1}$), 570 nm ($\varepsilon$ = 450 $M^{-1}.cm^{-1}$) and 430nm ($\varepsilon$ = 1095 $M^{-1}.cm^{-1}$) that are significantly different compared to the spectrum recorded in acetonitrile used for its preparation (Figure 1). In particular, the presence of transitions in the NIR region was already observed for fully delocalized **[1]** and **[2]** (1115 nm ($\varepsilon$ = 1190 $M^{-1}.cm^{-1}$) and 1255 nm ($\varepsilon$ = 690 $M^{-1}.cm^{-1}$), respectively, Figure S1). This result indicates clear structure changes upon dissolution in that case, with the formation of a new species denoted **[5]** that needs to be investigated.

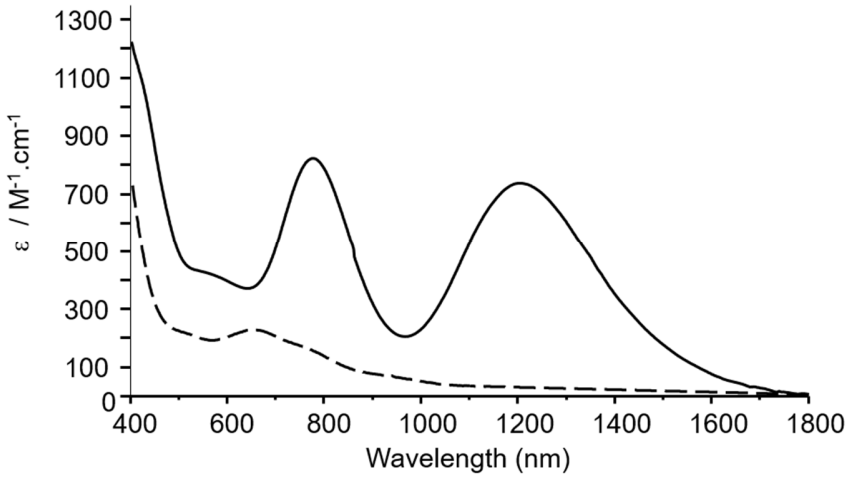


**Figure 1.** UV-vis/NIR spectra of **[3]** recorded in acetone (black solid, corresponding to **[5]**) and acetonitrile (black dashed, corresponding to **[4]**) at 298 K.

Spectral analogies between **[5]** and **[2]** strongly suggested, as working hypothesis, the presence of coordinated water molecule(s). **[2]** was indeed isolated upon reaction of the same $L^{Me(MAM)S\text{-}S}$ ligand and $[Cu(CH_3CN)_4](OTf)$ in acetone, the latter being more than likely the water source. Indeed, titration with 1,4-diazabicyclo[2.2.2] (DABCO) up to one molar equivalent resulted in drastic changes on the absorption spectrum (Figure S2). As a control experiment, no changes occurred upon addition of DABCO to an acetonitrile solution of **[4]** (Figure S3) that corresponds to solvated-**[3]** in acetonitrile.[11a] Consequently, a structure for **[5]** in which one copper would be coordinated by an acetonitrile exogenous ligand and the other one by a water molecule is a rational hypothesis ($Cu\text{-}OH_2$ converted into Cu-OH upon deprotonation). This new structure was successfully DFT-optimized (Figure 2, left) and showed, as for **[1]**, **[2]** and **[3]**, the presence of a Cu-Cu bond (2.7 Å) that was further confirmed by Natural Bond Order analysis (NBO, Figure 2, middle).

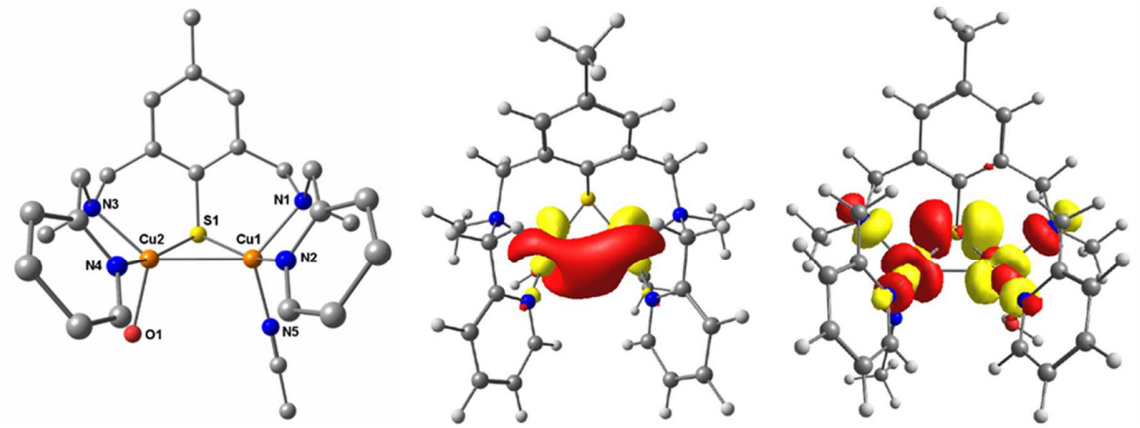


**Figure 2.** (left) Optimized structure of **[5]**; selected interatomic distances (Å) and angles(°): Cu1-Cu2, 2.703; Cu1-S1, 2.236; Cu1-N1, 2.083; Cu1-N2, 1.977; Cu1-N5, 2.029; Cu2-S1, 2.197; Cu2-N3, 2.059; Cu2-N4, 1.953; Cu2-O1, 2.158; Cu1-S-Cu2, 75.15 (see Table S1 in the Supporting Information for additional metric details); (middle) occupied natural orbital relevant to the Cu–Cu bond; (right) localized SOMO.

Each copper is pentacoordinated with two nitrogen atoms from the ligand (N1/N2 for Cu1 and N3/N4 for Cu2), the bridging thiophenolate (S1), one vicinal copper ion and either one oxygen (O1) or an extra nitrogen atom (N5) from a water or an acetonitrile molecule, respectively. For both, the geometry is best described as distorted tetragonal ($\tau_{Cu1} = 0.28$ and $\tau_{Cu2} = 0.27$).[12] Mülliken population analysis indicates closely distributed spin densities between Cu1 (0.24), Cu2 (0.26) and S1 (0.25) that account for 75% of the total. The remaining (25%) is spread over the pyridine rings (Figure S4 for the spin density plot). The localized Singly Occupied Molecular Orbital (SOMO, Figure 2, right) displays 56% Cu and 20% S character and shows a σ-antibonding interaction between the Cu $3dz^2$ orbitals and the S 3px orbital. A non-negligible degree of covalence for the Cu–S bond is expected due to the contribution of the S atom in the SOMO. For comparison, the distributed spin densities calculated for **[2]** are 0.27 (Cu1), 0.27 (Cu2) and 0.23 (S), and the spreading between Cu's and S (77%). This indicates that chemical modification at one metal center does not affect the spin distribution.

The calculated electronic excitations at 1200 nm, 763 nm, 693 nm and 496 nm obtained by TDDFT for optimized **[5]** are now in good agreement with the experiment (multi-peak analysis, 1222 nm, 776 nm, 630 nm, 560 nm, Figure S5). The nature of the transitions is finally assigned to intervalence (IVCT, CuS→CuS, NIR) and ligand to metal (LMCT) charge transfer processes (Figure S6).

Examination of **[5]** by EPR spectroscopy (Figure 3 and Figure S7) evidenced an interesting temperature dependence behavior. Up to 120K, the spectra are indicative of a valence-localized S = ½ system ($g_1$ = 2.201, $g_2$ = 2.066, $g_3$ = 2.036, $g_{iso}$ = 2.101; $A_{1Cu}$ = 545 MHz, $A_{2Cu}$ = 64 MHz, $A_{3Cu}$ = 10 MHz and $A_{iso}$ = 206 MHz) with a four lines pattern ($I_{Cu}$ = 3/2, 2n$I$+1 = 4 with n = 1). Going to 292K results in drastic changes with a more complicated multi-lines signature that resembles the one previously detected for fully delocalized **[1]** and **[2]**. **[5]** can thus be considered as a unique example of $Cu_2S$-containing MV species belonging to the class II category according to the Robin and Day classification.[13] Independently, the spectrum recorded upon addition of one molar eq. of DABCO at 10 K also differs from that of **[5]**, confirming the presence of a coordinating water ligand. The parameters ($g_1$ = 2.224, $g_2$ = 2.074, $g_3$ = 2.042 and $g_{iso}$ = 2.113; $A_{1Cu}$ = 582 MHz, $A_{2Cu}$ = 98 MHz, $A_{3Cu}$ = 10 MHz, $A_{iso}$ = 230 MHz, Figure S8) are again in that case close to the analog generated with **[2]** under the same conditions ($g_1$ = 2.180, $g_2$ = 2.050, $g_3$ = 2.012, $g_{iso}$ = 2.08; $A_{1Cu}$ = 535 MHz, $A_{2Cu}$ = 150 MHz, $A_{3Cu}$ = 10 MHz, $A_{iso}$ = 232 MHz, Figure S9). These parameters correlate well with the computed ones performed on DFT optimized structures considering a $Cu^{II}$-OH structure for both deprotonated **[2]** and **[5]** (Figures S10 and S11). Given the localized

character, no significant difference would have been expected since in both cases the $Cu^{II}$-OH motifs have identical chemical environments provided by the ligand.

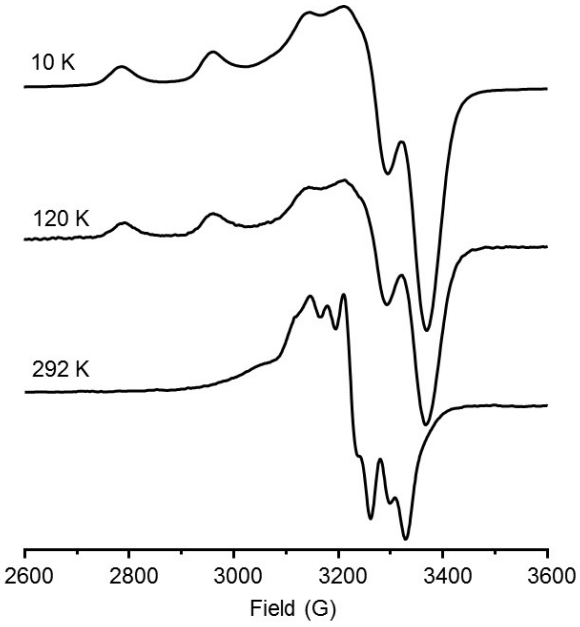


**Figure 3.** X-band EPR spectra of **[5]** recorded at 10 K, 120 K and 292 K in acetone.

Finally, the cyclic voltammogram (CV) recorded for **[5]** in acetone displays two distinct quasi-reversible redox processes (Figure 4). The first one ($E_{pa1}$ = -90 mV, $E_{pc1}$ = -250 mV, ΔEp = 160 mV, $E_{1/2}$ = -170 mV vs $Fc^{+/0}$) is assigned to a $Cu_2^{I,I} \rightarrow Cu_2^{II,I}$ system and the second ($E_{pa2}$ = 335 mV, $E_{pc2}$ = 195 mV, ΔEp = 140 mV, $E_{1/2}$ = 265 mV) to $Cu_2^{II,I} \rightarrow Cu_2^{II,II}$. The CV has similarities compared to that of **[2]** with the Cu-Cu bond and N/O environment but differs from **[3]** and **[4]** with exclusive N-coordinating atoms and (or not) Cu-Cu bond (Figure S12). The electronic communication within the cores that relies on the $Cu_2S$ triangle motif is thus highly sensitive to the

environment. The anodic system is the most affected, with higher redox potential in presence of the metal-metal bond that tends to stabilize the MV state over a larger potential range.

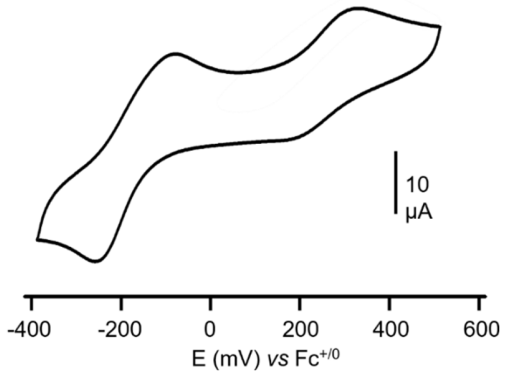


**Figure 4.** Cyclic voltammogram of **[5]** in acetone with 0.1 M $Bu_4N(ClO_4)$ as supporting electrolyte and glassy carbon as working electrode. The curve corresponds to the n+1 scan at 100 $mV.s^{-1}$.

The molecular structure of **[5]** in acetone being established, its $N_2O$r activity was investigated using UV-vis, EPR, ESI-MS and gas chromatography (GC) methods. Interestingly, while **[3]** (in dichloromethane) and **[4]** (in acetonitrile) are completely unreactive, noticeable changes are detected by absorption spectroscopy upon $N_2O$ bubbling into an acetone solution of **[5]** (Figure 5).

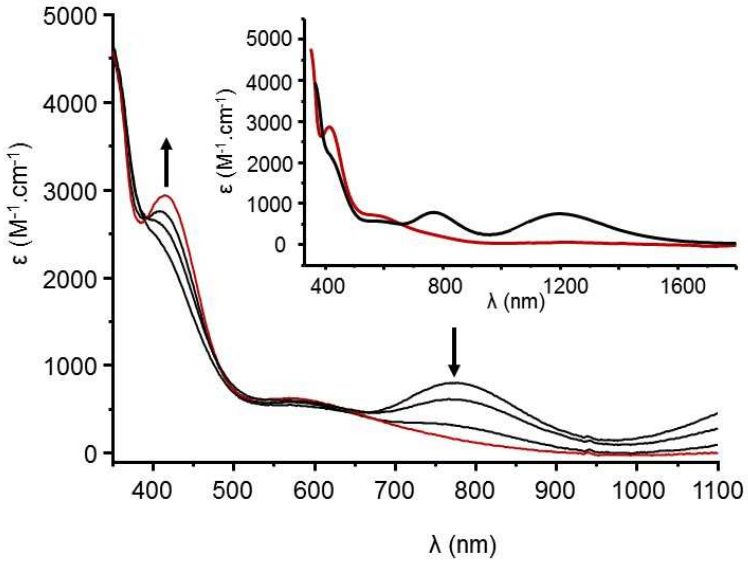


**Figure 5.** UV-vis monitoring of the conversion of **[5]** (solid black to red) upon $N_2O$ bubbling in acetone (0 to 10 min) and (insert) full UV-vis/NIR spectra of **[5]** (solid black) and the final species (solid red).

While the two main absorption bands at 1205 nm and 775 nm vanished within 10 minutes, a new feature is detected at 415 nm. The presence of an isosbestic point at 390 nm indicates the consumption of the starting complex and its clean conversion into a new species without side reactions. This behavior was already evidences for **[2]**, unique $Cu_2S$ MV reported at that time for single turnover $N_2O$ reduction at room temperature. An EPR and ESI-MS follow-up of the reaction gave additional information about redox character of the reaction (Figure S13). Indeed, the axial S= ½ signal characteristic of **[5]** gradually disappeared concomitantly with $N_2O$ bubbling and a +2 net charge fragment consistent with the integrity of the organic framework, two Cu(II) ions and the presence of an hydroxo ligand (Figure S14) are observed. These results are thus consistent with the formation of a dinuclear Cu(II) complex with an hydroxo bridge that confers the required

antiferromagnetic coupling to silent the EPR signal. Additionally, examination of the headspace gas gave clear evidence about $N_2$ formation and confirms $N_2O$ reduction (Figure S15). A reaction rate order for **[5]** of 0.77 ± 0.02 under *pseudo*-first order conditions was determined (Figure S16), suggesting (as for **[2]**) the involvement of a reaction intermediate that consumes **[5]** along the reaction (since a two-electron process is required for the reduction). Finally, the reaction rate was calculated to be 83 ± 3 $min^{-1}$ whereas 8.0 ± 0.1 $min^{-1}$ was obtained for **[2]** (Figure S17). This result is important form a structure/activity correlation point of view. Since the *aquo* species are the only active ones, the coordination sphere of the adjacent Cu center has a non-negligible effect on the reaction rate and is now a new parameter to be considered. In addition, for **[2]**, a stabilizing H-bond between the water and triflate ligands could also explain such differences in reactivity.

## CONCLUSION

In summary, a new dinuclear MV copper complex **[5]** containing an opened $Cu_2S$ core with acetonitrile and water molecules as exogenous ligands was generated upon dissolution of a bis($CH_3CN$) precursor **[3]** in acetone and fully characterized. The DFT-optimized structure is analogous to that of the other *aqua* parent **[2**], with the presence of a Cu-Cu bond. The electronic structure was probed by TDDFT methods and the NIR band connected to IVCT. **[5]** has an original (unique in this series and not observed for **[2]** with the ($H_2O$)Cu-Cu(OTf) motif.) EPR temperature dependence behavior with a localized valence at least between 10 K and 120 K and a delocalized

character at 292 K  The electrochemical behavior of **[5]** reminds that of **[2]** and differs from the other members of the series where the water ligand and (or) the Cu-Cu bond (is) are missing (**[3]** and **[4]**). Even more interesting was the detection of a $N_2Or$ activity that led us to attest for the importance of a Cu-$OH_2$ moiety when targeting such a reactivity, and corroborates the results obtained for **[2]**. Finally, the kinetic data indicate *(i)* a rate order under *pseudo*-first order conditions close to 1 in agreement with the participation of a reaction intermediate that consumes **[5]** to promote the two-electron reduction process and *(ii)* a reaction rate 10 times faster compared to **[2]**. This result is of main interest for establishing a rationale for $N_2O$ activation with these bio-inspired systems. Indeed, not only the Cu-$OH_2$ part is essential, but also the coordination sphere of the adjacent Cu center influences the reaction. For **[5]** the $_3NCuSCuN_2O_1$ motif reminds that of the dissymmetric $Cu_ICu_{IV}$ edge at $Cu_Z^*$ with exclusively nitrogen atoms in addition to the oxygen form water. This chemical environment could be the common determinant for an efficient reactivity. Experiments to prepare *(i)* new complexes combining various Cu-X spheres and the Cu-$OH_2$ motif to confirm these result and *(ii)* derivatives lacking de Cu-Cu bond but still having the Cu-$OH_2$ motif, which would to help in evaluating the influence of this structural feature on the reactivity and currently performed.

## ASSOCIATED CONTENT

### Supporting Information

Full descriptions of materials and methods, DFT-optimized structure of **[5]**, electronic structure of **[5]**; DFT-optimized structure of deprotonated **[5]** and **[2]**, experimental and simulated EPR spectra, ESI-MS data, GC-MS profile for $N_2$ detection, kinetic data.

## AUTHOR INFORMATION


### Corresponding Author

*Email: stephane.torelli@cea.fr

### ORCID

Stéphane Torelli 0000-0001-7530-8120


### Notes

The authors declare no competing financial interests

## ACKNOWLEDGMENTS


The authors gratefully acknowledge the Labex ARCANE and the CBH-EUR-GS (ANR-17-EURE-0003) fund for their partial financial support *via* the CNRS, CEA, and the University of Grenoble-Alpes. We are grateful to Colette Lebrun for her precious assistance in recording ESI-mass spectra and to Bernard Sartor for technical assistance.

## REFERENCES


1. (a) B. Bates; Z. W. Kundzewicz; S. Wu, N. A., V. Burkett, P. Döll, D. Gwary, C. Hanson, B. Heij, B. Jiménez, G. Kaser, A. Kitoh, S. Kovats, P. Kumar, C. Magadza, D. Martino, L. J. Mata, M. Medany, K. Miller, T. Oki, B. Osman, J. Palutikof, T. Prowse, R. Pulwarty, J. Räisänen, J. Renwick, F. Tubiello, R. Wood, Z.-C. Zhao, J. Arblaster, R. Betts, A. Dai, C. Milly, L. Mortsch, L. Nurse, R. Payne, I. Pinskwar,; Wilbanks, T., *Technical Paper on Climate Change and Water* **2008,** *ed. I. Secretariat*; (b) Solomon, S.; Qin, D.; Manning, M.; Chen, Z.; Marquis, M.; Averyt, K.; Tignor, M. M. B.; Miller, H. L., *Contribution of Working Group I to the fourth Assessment report of the Intergovernmental Panel on climate Change, 2007;*. Cambridge University Press: Cambridge, UK, 2007; (c) Richardson, D.; Felgate, H.; Watmough, N.; Thomson, A.; Baggs, E., Mitigating release of the potent greenhouse gas N2O from the nitrogen cycle – could enzymic regulation hold the key? *Trends Biotechnol.* **2009,** *27* (7), 388-397; (d) Ravishankara, A. R.; Daniel, J. S.; Portmann, R. W., Nitrous Oxide (N2O): The Dominant Ozone-Depleting Substance Emitted in the 21st Century. *Science* **2009,** *326* (5949), 123-125.
2. Sanders, R. D.; Weimann, J.; Maze, M., Biologic Effects of Nitrous OxideA Mechanistic and Toxicologic Review. *Anesthesiology* **2008,** *109* (4), 707-722.
3. Deacon, R.; Lumb, M.; Perry, J.; Chanarin, I.; Minty, B.; Halsey, M.; Nunn, J., Inactivation of Methionine Synthase by Nitrous Oxide. *Eur. J. Biochem.* **1980,** *104* (2), 419-422.
4. Hoerauf, K.; Lierz, M.; Wiesner, G.; Schroegendorfer, K.; Lierz, P.; Spacek, A.; Brunnberg, L.; Nüsse, M., Genetic damage in operating room personnel exposed to isoflurane and nitrous oxide. *Occup. Environ. Med.* **1999,** *56* (7), 433-437.
5. Jevtovic-Todorovic, V.; Benshoff, N.; Olney, J. W., Ketamine potentiates cerebrocortical damage induced by the common anaesthetic agent nitrous oxide in adult rats. *Br. J. Pharmacol.* **2000,** *130* (7), 1692-1698.
6. Pauleta, S. R.; Dell'Acqua, S.; Moura, I., Nitrous oxide reductase. *Coord. Chem. Rev.* **2013,** *257* (2), 332-349.
7. (a) Brown, K.; Djinovic-Carugo, K.; Haltia, T.; Cabrito, I.; Saraste, M.; Moura, J. J. G.; Moura, I.; Tegoni, M.; Cambillau, C., Revisiting the catalytic CuZ cluster of nitrous oxide (N2O) reductase - Evidence of a bridging inorganic sulfur. *J. Biol. Chem.* **2000,** *275* (52), 41133-41136; (b) Pomowski, A.; Zumft, W. G.; Kroneck, P. M. H.; Einsle, O., N2O binding at a [lsqb]4Cu:2S[rsqb] copper-sulphur cluster in nitrous oxide reductase. *Nature* **2011,** *477* (7363), 234-237.
8. (a) Gorelsky, S. I.; Ghosh, S.; Solomon, E. I., Mechanism of N2O Reduction by the Tetranuclear CuZ Cluster of Nitrous Oxide Reductase. *J. Am. Chem. Soc.* **2006,** *128* (1), 278-290; (b) Solomon, E.; Sarangi, R.; Woertink, J.; Augustine, A.; Yoon, J.; Ghosh, S., O2 and N2O Activation by Bi-,Tri-, and Tetranuclear Cu Clusters in Biology. *Acc.Chem.Res.* **2007,** *40*, 581-591; (c) Ghosh, S.; Gorelsky, S. I.; DeBeer George, S.; Chan, J. M.; Cabrito, I.; Dooley, D. M.; Moura, J. J. G.; Moura, I.; Solomon, E. I., Spectroscopic, Computational, and Kinetic Studies of the *í*4-Sulfide-Bridged Tetranuclear CuZ Cluster in N2O Reductase: pH Effect on the Edge Ligand and Its Contribution to Reactivity. *J. Am. Chem. Soc.* **2007,** *129*, 3955-3965; (d) Johnston, E. M.; Dell'Acqua, S.; Ramos, S.; Pauleta, S. R.; Moura, I.; Solomon, E. I., Determination of the Active Form of the Tetranuclear Copper Sulfur Cluster in Nitrous Oxide Reductase. *J. Am. Chem. Soc.* **2013,** *136* (2), 614-617; (e) Johnston, E. M.; Dell'Acqua, S.; Pauleta, S. R.; Moura, I.; Solomon, E. I., Protonation state of the Cu4S2 CuZ site in nitrous oxide reductase: redox dependence and insight into reactivity. *Chem. Sci.* **2015,** *6* (10), 5670-5679.
9. Johnston, E. M.; Carreira, C.; Dell'Acqua, S.; Dey, S. G.; Pauleta, S. R.; Moura, I.; Solomon, E. I., Spectroscopic Definition of the CuZ° Intermediate in Turnover of Nitrous Oxide Reductase and Molecular Insight into the Catalytic Mechanism. *J. Am. Chem. Soc.* **2017,** *139* (12), 4462-4476.
10. (a) Bar-Nahum, I.; Gupta, A. K.; Huber, S. M.; Ertem, M. Z.; Cramer, C. J.; Tolman, W. B., Reduction of Nitrous Oxide to Dinitrogen by a Mixed Valent Tricopper-Disulfido Cluster. *J. Am. Chem. Soc.* **2009,** *131*, 2812-2814; (b) Johnson, B. J.; Antholine, W. E.; Lindeman, S. V.; Mankad, N. P., A Cu4S model for the nitrous oxide reductase active sites supported only by nitrogen ligands. *Chem. Commun.* **2015,** *51* (59), 11860-11863; (c) Johnson, B. J.; Antholine, W. E.; Lindeman, S. V.; Graham, M. J.; Mankad, N. P., A One-Hole Cu4S Cluster with N2O Reductase Activity: A Structural and Functional Model for CuZ*. *J. Am. Chem. Soc.* **2016,** *138* (40), 13107-13110; (d) Bagherzadeh, S.; Mankad, N. P., Oxidation of a [Cu2S] complex by N2O

and CO2: insights into a role of tetranuclearity in the CuZ site of nitrous oxide reductase. *Chem. Commun.* **2018,** *54* (9), 1097-1100.

11. (a) Esmieu, C.; Orio, M.; Mangue, J.; Pécaut, J.; Ménage, S.; Torelli, S., Valence Localization at a Bio-inspired Mixed-Valent {Cu2S}2+ Motif upon Solvation in Acetonitrile: Effect on Nitrous Oxide Reductase (N2Or) Activity. *Chem. Eur. J.* **2018,** *24* (20), 5060-5063; (b) Esmieu, C.; Orio, M.; Torelli, S.; Le Pape, L.; Pecaut, J.; Lebrun, C.; Menage, S., N2O reduction at a dissymmetric {Cu2S}-containing mixed-valent center. *Chem. Sci.* **2014,** *5* (12), 4774-4784; (c) Torelli, S.; Orio, M.; Pécaut, J.; Jamet, H.; Le Pape, L.; Ménage, S., A {Cu2S}2+ Mixed-Valent Core Featuring a Cu-Cu Bond. *Angew. Chem. Int. Ed.* **2010,** *49* (44), 8249-8252.
12. Addison, A. W.; Rao, T. N.; Reedijk, J.; van Rijn, J.; Verschoor, G. C., *J. Chem. Soc., Dalton Trans.* **1984**, 1349.
13. (a) Day, P.; Hush, N. S.; Clark, R. J. H., Mixed valence: origins and developments. *Phil. Trans. R. Soc. A* **2008,** *366* (1862), 5-14; (b) Robin, M.; Peter, D., Mixed Valence Chemistry. *Adv. Inorg. Chem. Radiochem* **1967,** *10*, 247-422.